scientific reports

Check for updates

OPEN

Spin-glass transition in the spin–orbit-entangled $J_{eff}=0$ Mott insulating double-perovskite ruthenate

Hayato Yatsuzuka[1], Yuya Haraguchi[1]✉, Akira Matsuo[2], Koichi Kindo[2] & Hiroko Aruga Katori[1,3]

We have successfully synthesized new Ru^{4+} double perovskite oxides $SrLaInRuO_6$ and $SrLaGaRuO_6$, which are expected to be a spin–orbit coupled $J_{eff}=0$ Mott insulating ground state. Their magnetic susceptibility is much significant than that expected for a single Ru^{4+} ion for which exchange coupling with other ions is negligible. Their isothermal magnetization process suggests that there are about 20 percent isolated spins. These origins would be the Ru^{3+}/Ru^{5+} magnetic defects, while the regular Ru^{4+} sites remain nonmagnetic. Moreover, $SrLaGaRuO_6$ shows a spin-glass-like magnetic transition at low temperatures, probably caused by isolated spins. The observed spin-glass can be interpreted by the analogy of a dilute magnetic alloy, which can be seen as a precursor to the mobile $J_{eff}=1$ exciton as a dispersive mode as predicted.

Recent material investigations have revealed novel phenomena driven by spin–orbit coupling (SOC)[1–20]. The strong SOC splits a t_{2g} band into $J=3/2$ and $J=1/2$ bands, which results in the realization of the SOC Mott insulating state. For example, the Ir^{4+} ions with the d^5 electron configuration have an effective orbital moment $L=1$, resulting in a $J_{eff}=1/2$ pseudospin. Such a spin–orbit-entanglement gives rise to unconventional interaction among pseudospins. In the case of $J_{eff}=1/2$ pseudospins, the bond-dependent Ising interactions, which have been called the Kitaev interaction in recent years, are realized[1]. Such a realization of the SOC pseudospin state was first observed in layered perovskite Sr_2IrO_4[2]. Consequently, it is theoretically predicted that a honeycomb lattice magnet with $J_{eff}=1/2$ pseudospins is a promising host of a quantum spin liquid (QSL). In the realistic compounds, $RuCl_3$ and $H_3LiIr_2O_6$ exhibit the Kitaev QSL behavior[3–6].

In contrast, the d^4 electron system (Ru^{4+}, Os^{4+}, and Ir^{5+}) has not been attracted much attention due to an absence of local moments in the ionic ground state. However, $J_{eff}=1$ excitations become dispersive modes in a crystal due to moderate superexchange (SE) interactions. These mobile spin–orbit excitons may condense in this situation, which results in a magnetically ordered state[7–10]. In order to realize such a state, the exchange interaction must overcome a critical value sufficient to exceed the energy gap Δ between the $J_{eff}=0$ and $J_{eff}=1$[7,11,12]. Such a condensed state, for which the physicists conceive a terminology—spin–orbit-exciton condensation (SOEC), is analogous to magnon condensation phenomena in a spin dimer system[13]. One factor differentiating the d^4 system from the spin-dimer one is the anisotropy of the strong exchange interaction, which originates from the strong spin–orbit interaction. Therefore, it is expected that a novel condensed phase will be realized.

Although theoretical studies have been enormously advanced to search for anomalous phenomena driven by SOEC, experimental studies have not been carried out due to the lack of model materials. This situation is because the energy scale of Δ is too large; the $5d^4$ (Ir^{5+} and Os^{4+}) compounds should be typically nonmagnetic. Indeed, the weak magnetic anomalies observed in some Ir^{5+} double perovskites are better explained by the Ir^{4+} and Ir^{6+} magnetic defects rather than SOEC[14–21]. Therefore, a SOEC seems to be much less feasible for $5d$ compounds. On the other hand, SOEC is more likely realizable in $4d^4$ compounds such as Ru^{4+}, where SOC is smaller than Ir^{5+} and is comparable to SE. Moreover, the SOC vs. SE competition can be tuned by a lattice control. Therefore, Ru^{4+} double perovskites would be good model-compounds for a realization of SOEC[22].

We report the magnetic properties of novel double perovskites $SrLaInRuO_6$ and $SrLaGaRuO_6$ with Ru^{4+} ion. These deviate significantly from the single-spin susceptibility expected for Ru^{4+} ($J_{eff}=0$) ions, even though the

[1]Department of Applied Physics, Tokyo University of Agriculture and Technology, Koganei, Tokyo 184-8588, Japan. [2]The Institute for Solid State Physics, The University of Tokyo, Kashiwa, Chiba 277-8581, Japan. [3]Research Center for Thermal and Entropic Science, Graduate School of Science, Osaka University, Toyonaka, Osaka 560-0043, Japan. ✉email: chiyuya3@go.tuat.ac.jp

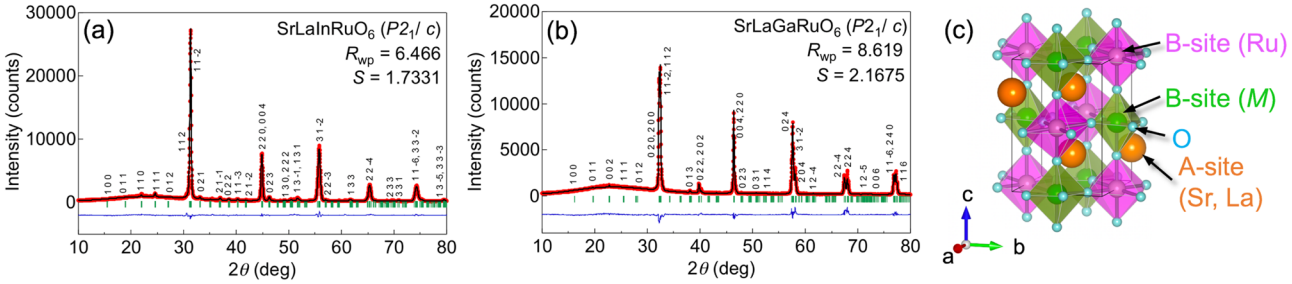

Figure 1. Powder X-ray diffraction patterns of (**a**) $SrLaInRuO_6$ and (**b**) $SrLaGaRuO_6$. The observed intensities (red), calculated intensities (black), and their differences (blue) are shown. Vertical bars (green) indicate the positions of the Bragg reflections. (**c**) Crystal structure of $SrLaMRuO_6$ (M = In, Ga) obtained from crystal structure parameters refined using the Rietveld method. The VESTA program is used for visualization[24].

atom	site	x	y	z	B (Å)
$SrLaInRuO_6$					
Sr/La	4e	0.5060 (7)	0.5346 (3)	0.252 (1)	0.23 (4)
In	2c	0	1/2	0	1.3 (3)
Ru	2b	1/2	0	0	1.3 (3)
O1	4e	0.229 (7)	0.222 (7)	0.992 (6)	2.7 (2)
O2	4e	0.324 (7)	0.704 (6)	0.963 (4)	2.7 (2)
O3	4e	0.405 (5)	0.988 (2)	0.222 (5)	2.7 (2)
$SrLaGaRuO_6$					
Sr/La	4e	0.4999 (3)	0.498 (3)	0.2492 (9)	0.10 (4)
Ga	2c	0	1/2	0	0.97 (7)
Ru	2b	1/2	0	0	0.97 (7)
O1	4e	0.24 (1)	0.241 (7)	1.007 (6)	2.2 (2)
O2	4e	0.328 (8)	0.676 (5)	1.028 (3)	2.2 (2)
O3	4e	0.50 (2)	0.99 (2)	0.250 (4)	2.2 (2)

Table 1. Crystallographic parameters for $SrLaInRuO_6$ and $SrLaGaRuO_6$ (both space group: $P2_1/c$) determined from powder X-ray diffraction experiments. The obtained lattice parameters are $a = 5.6976$ (4), $b = 5.7427$ (4), $c = 8.0669$ (5) Å, and $\beta = 90.05$ (1)° for $SrLaInRuO_6$, and $a = 5.5077$ (4), $b = 5.5538(3)$, $c = 7.8210$ (3) Å, and $\beta = 90.586$ (3)° for $SrLaGaRuO_6$. B is the atomic displacement parameter.

distance between the magnetic ions is sufficiently large. Furthermore, the magnetization process up to 60 T demonstrates the presence of about 20 percent isolated spins. These behaviors can be explained as originating from the Ru^{3+}/Ru^{5+} magnetic defects. Moreover, only $SrLaGaRuO_6$ shows a spin-glass transition at $T_f \sim 50$ K. We discuss the origin of the observed spin-glass transition from the analogy of the dilute magnetic alloy from the viewpoint of $J_{eff} = 0$ physics in SOC Mott insulators.

Experimental methods

Polycrystalline samples of $SrLaMRuO_6$ (M = In, Ga) were synthesized by the conventional solid-state reaction from stoichiometric mixtures of $SrCO_3$, La_2O_3, M_2O_3 (M = In, Ga), and RuO_2. The obtained samples were characterized by powder X-ray diffraction (XRD) measurements using a diffractometer with Cu $K\alpha$ radiation. The cell and crystal structure parameters were refined using the Rietveld method using RIETAN-FP version 2.16 software[23]. The temperature dependence of the magnetization was measured using the magnetic property measurement system (MPMS; Quantum Design) equipped in the Institute for Solid State Physics at the University of Tokyo. Magnetization curves up to 60 T were measured using an induction method with a multilayer pulsed magnet at the Institute for Solid State Physics at the University of Tokyo.

Results

Crystal structure. Figure 1a and b shows powder XRD patterns from thus-obtained samples. All peaks are indexed to monoclinic unit cells based on the space group of $P2_1/c$. The Rietveld analysis converged well with the distorted double perovskite structure shown in Fig. 1c and the structural parameters in Table 1. No deviation from the ratio of Sr:La = 1:1 was detected within the experimental error. We estimate the modified tolerance factor t_m as structural stability in double perovskite using the ionic radii values, yielding $t_m = 0.93834$ and 0.98015 in $SrLaInRuO_6$ and $SrLaGaRuO_6$, respectively. In the condition of $t_m < 1$, the double perovskite-type compounds should crystallize a monoclinic structure[25,26]. Our samples certainly satisfy the criterion.

Formula	cation	Bond valence sum
$SrLaInRuO_6$	In^{3+}	+2.838
	Ru^{4+}	+4.352
$SrLaGaRuO_6$	Ga^{3+}	+2.944
	Ru^{4+}	+4.056

Table 2. Calculation of the bond valence sum (B_V) for the octahedron in $SrLaInRuO_6$ and $SrLaGaRuO_6$.

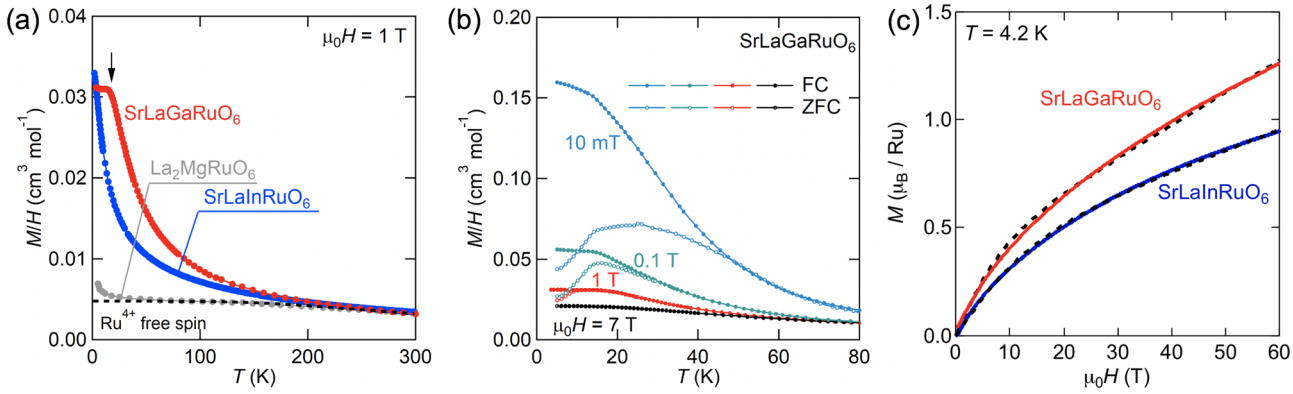

Figure 2. (**a**) Temperature dependence of magnetic susceptibility M/H of $SrLaMRuO_6$ (M = In, Ga) and La_2MgRuO_6[28,29] under a magnetic field of 1 T. In this figure, only the results of field cooling (FC) data are shown. The black dotted curve shows the free-spin magnetization of Ru^{4+} ions calculated as described in the text. (**b**) The M/H curves of $SrLaGaRuO_6$ under several magnetic fields. In each field, measurements were conducted upon heating after zero-field cooling (ZFC, open circles) and then upon cooling (FC, closed circles). (**c**) The isothermal magnetization of $SrLaInRuO_6$ and $SrLaGaRuO_6$ under a magnetic field up to 60 T at 4.2 K. The black dashed lines represent the best fit by Eq. (4) described in the text.

In estimating the valence of the B-site cations at the center of the octahedral MO_6 (M = In, Ga) and RuO_6 in the two double perovskite oxides, we used the bond valence sum B_V expressed by the following formula[27],

$$B_V = \sum_i^N \exp\left(\frac{R_0 - R_i}{0.37}\right) \tag{1}$$

where R_0 is the empirical bonding parameter, R_i is the inter-bond cation–anion distance, and N is the coordination number. The estimated B_V values of In/Ga and Ru ions in $SrLaInRuO_6$ and $SrLaGaRuO_6$ are listed in Table 2, which aligns with the expected values.

Magnetism. Figure 2a shows the temperature dependence of magnetization M/H of $SrLaMRuO_6$ (M = In, Ga) under an applied field of 1 T. For comparison, the M/H data of La_2MgRuO_6[28,29] with a similar d^4 electron configuration is displayed. The magnetic response of $SrLaMRuO_6$ and La_2MgRuO_6 is quite different despite the similar electronic state of the Ru^{4+} single ion. When considered from a crystallographic point of view, these compounds are not expected to have strong magnetic interactions because of the significant separation of Ru^{4+} ions. Therefore, it seems strange that the magnetic responses of $SrLaMRuO_6$ and La_2MgRuO_6 are so different. Kotani theoretically predicted the effective magnetic moment of d^n ions ($n = 1 \sim 5$) as a function of electron filling n, spin–orbit coupling, temperature, and ligand environment[30]. The effective magnetic moment $\mu_{eff}(T)$ of low-spin d^4 in an octahedral environment can be expressed as follows,

$$\mu_{\mathrm{eff}}{}^2 = \frac{3\left[24+(x/2-9)e^{-x/2}+(5x/2-15)e^{-3x/2}\right]}{x\left[1+3e^{-x/2}+5e^{-3x/2}\right]} \tag{2}$$

where $x = \lambda/k_BT$, λ is the spin–orbit coupling interaction[30], and k_B is the Boltzmann constant. Thus, the magnetic susceptibility of isolated Ru^{4+} ions χ_{calc} can be expressed as follows,

$$\chi_{\mathrm{calc}} = \frac{N\mu_{\mathrm{eff}}{}^2}{3k_BT} \tag{3}$$

The dotted black curve in Fig. 2a represents the χ_{calc} curve calculated using a value of $\lambda = 980\ cm^{-1}$ for Ru^{4+} ions. The λ-value is expected to be smaller than the completely free-ion value of $\lambda = 1400\ cm^{-1}$ determined in the study used Ru^{4+} complexes[31], which origin of λ-shrinking would be covalency. Note that it is necessary to incorporate the effect of the low symmetry field in order to reproduce the susceptibility in distorted Ru^{4+} double perovskites since Eq. (2) is calculated in the cubic symmetry field. The M/H data of La_2MgRuO_6 seemingly

	$N_{1/2}$ (Ru^{5+})	$N_{3/2}$ (Ru^{3+})	χ_{vv} (cm^3/mol Oe)
$SrLaInRuO_6$	0.1088 (3)	0.1088 (3)	0.00869 (2)
$SrLaGaRuO_6$	0.0937 (21)	0.0937 (21)	0.01503 (2)

Table 3. Results of fits to the isothermal M using the model described in the text. The parameters $N_{1/2}$ and $N_{3/2}$ are fixed to equal.

follows χ_{calc}, while those of $SrLaMRuO_6$ significantly deviate from χ_{calc}. This fact indicates that the Ru^{4+} ions in $SrLaMRuO_6$ are not simply in the $J_{eff}=0$ ground state.

Both M/H data for $SrLaMRuO_6$ are in the rough agreement above 250 K, but below 250 K, are greatly enhanced compared to the χ_{calc} curve. In Ir^{5+} double perovskites, in which a similar $J_{eff}=0$ ground state is expected, the M/H data of Sr_2YIrO_6 shows almost temperature-independent behavior[21]. On the other hand, a similar enhancement in low-temperature M/H data is observed in the solid solution system $Sr_{2-x}Ca_xYIrO_6$[21]. Therefore, this increase in magnetization may affect randomness, of which a mechanism will be discussed later.

Moreover, $SrLaGaRuO_6$ shows a magnetic anomaly at low temperatures (displayed by an arrow in Fig. 2a), contrasting with no anomaly in $SrLaInRuO_6$. Figure 2b expands the low-temperature region under magnetic fields from 0.01 to 1 T. At the lowest field of 0.01 T, the M/H data exhibit an apparent thermal hysteresis between the zero-field-cooled (ZFC) and field-cooled (FC) data below $T_f \sim 50$ K. This hysteresis is suppressed by increasing the magnetic field and is eventually merged at 7 T. This behavior is a typical feature of spin-glass transition[32].

High-field magnetization. Figure 2c shows the isothermal magnetization M up to 60 T. The M-H curves show convex behavior upward, implying an isolated spin different from the van Vleck magnetism of Ru^{4+} pseudospin $J_{eff}=0$ state. The origin of the isolated spin will be discussed later. The increase in magnetization at high-field regions is due to the van Vleck paramagnetism.

Discussion

As described above, the two novel double perovskite ruthenates $SrLaInRuO_6$ and $SrLaGaRuO_6$ are expected to show a van Vleck magnetism of Ru^{4+} pseudospin $J_{eff}=0$ state. However, the observed M/H is considerably larger than a single Ru^{4+} spin, indicating the deviation from the $J_{eff}=0$ state. In addition, the isothermal magnetization demonstrates the existence of an isolated spin.

A similar enhancement of magnetization has been reported in highly solid-solution double perovskite iridates $Sr_{2-x}Ca_xYIrO_6$[21]. An X-ray magnetic circular dichroism (XMCD) measurement demonstrates an emergent partial charge disproportionation (PCD) of $Ir^{5+} \rightarrow 0.5Ir^{4+} + 0.5Ir^{6+}$ due to a site-randomness[21]. In light of this result, similar Ru^{3+}/Ru^{5+} magnetic defects possibly occurs in $SrLaInRuO_6$ and $SrLaGaRuO_6$ due to a similar intrinsic A-site randomness.

The magnetization of isolated spin M_{iso} follows a Brillouin function, while the van Vleck term M_{VV} should be proportional to H. Both terms would contribute to the observed nonlinear behaviors of the isothermal M. Here, in order to separate the contributions of the isolated spins and the van Vleck term, we analyze the M data with a modified Brillouin function,

$$M = M_{iso} + M_{vv} = \sum\nolimits_J N_J g_J \mu_B J \left\{ \frac{2J+1}{2J} \coth\left(\frac{2J+1}{2J} \frac{g_J \mu_B J H}{k_B T} \right) - \frac{1}{2J} \coth\left(\frac{1}{2J} \frac{g_J \mu_B J H}{k_B T} \right) \right\} + \chi_{vv} H \quad (4)$$

where N_J represents a scaling factor to account for a finite number of paramagnetic free spins, g_J (~ 2) is the g-factor, μ_B is the Bohr magneton, J (= 1/2 and 3/2) is the total angular momentum. For the second term, χ_{vv} indicates the van Vleck term. The values of N and χ_{vv} are summarized in Table 3. Provided that $N_{1/2}$ and $N_{3/2}$ are fixed to equal considering the local charge disproportionation model, the M data up to 60 T fit the Eq. (4). The best fits are shown by the dashed lines in Fig. 2c, with the fitting parameters given in Table 3. Our analysis suggests that ~ 20% of free spins (J = 1/2 and 3/2) are present. The orphan spins possibly emerged by the valence being off from tetravalent, which is no evidence from the crystal structural analysis. Although we cannot rule out other origins, these facts support that the PCD model is a good solution. As in the Ir^{5+} system, the PCD-generated isolated spins may be directly detected by XMCD measurements: it is a further issue. In addition, the van Vleck term was found to be more significant for $SrLaGaRuO_6$.

The estimated van Vleck term of $SrLaGaRuO_6$ is larger than $SrLaInRuO_6$. According to Boltzmann statistics, the van Vleck term is proportional to the concentration of $J_{eff}=1$ exciton. Therefore, the difference in χ_{vv} between $SrLaInRuO_6$ and $SrLaGaRuO_6$ is due to the different Δ. In the theoretical prediction, a non-cubic crystal field, generated by a distortion of the RuO_6 octahedra, effectively reduces Δ[33]. Here, we introduce the bond angle variance σ, as a scale parameter of the polyhedral distortion. The σ-value in the RuO_6 octahedra can be parametrized by the following formula,

$$\sigma = \sqrt{\sum\nolimits_{i=1}^{12} \frac{(\varphi_i - \varphi_0)^2}{m-1}} \quad (5)$$

where m is the number of O–Ru–O angles, φ_i is the ith bond angle of the distorted coordination-polyhedra, and φ_0 is the bond angle of the coordination polyhedral with O_h symmetry; φ_0 equals 90° for octahedron. Calculations

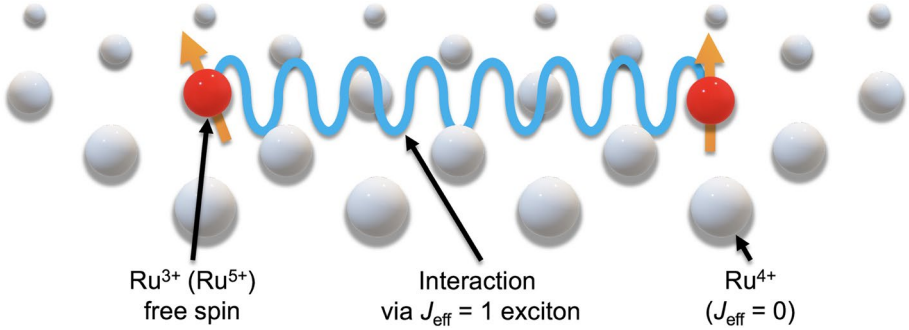

Figure 3. Schematic of the mechanism of spin-glass induced by isolated spin and $J_{\mathrm{eff}}=1$ excitons, as an analogy of a dilute magnetic alloy. The interaction between free spins mediated by mobile $J_{\mathrm{eff}}=1$ excitons corresponds to the RKKY interaction.

using the atomic position parameters listed in Table 1 yield the σ-values of 7.7976° and 10.2708° for $SrLaInRuO_6$ and $SrLaGaRuO_6$, respectively, indicating a strikingly larger non-cubic crystal field in $SrLaGaRuO_6$ than $SrLaInRuO_6$. Therefore, the concentration of $J_{\mathrm{eff}}=1$ exciton of $SrLaGaRuO_6$ should be larger than $SrLaInRuO_6$, consistent with the large-small relationship of χ_{vv}.

Furthermore, it is theoretically predicted that the SE interaction between $J_{\mathrm{eff}}=0$ reduces Δ. In $SrLaInRuO_6$ and $SrLaGaRuO_6$, the $J_{\mathrm{eff}}=0$ pseudospins interact via the SE interaction through Ru^{4+}–O^{2-}–M^{3+}–O^{2-}–Ru^{4+} paths with M = In, Ga. Thus, it is considered that the difference in the SE interaction between these two systems arises from the filled outermost orbitals, which are 4*d* and 3*d* orbitals for $SrLaInRuO_6$ and $SrLaGaRuO_6$, respectively. Therefore, it is reasonable that the SE magnitude is different.

Based on the results so far, it is reasonable to consider that the spin-glass transition in $SrLaGaRuO_6$ is due to randomly arranged isolated spins. Strangely enough, however, no spin-glass transition has been observed in $SrLaInRuO_6$, where the isolated spin concentration is comparable. However, it is unlikely that all the 19% localized spins interact strongly in $SrLaGaRuO_6$ where the Ru–Ru distance is far apart. This fact suggests a difference in the magnitude of the interaction between randomly arranged isolated spins.

The origin of the spin-glass transition in $SrLaGaRuO_6$ can be inferred by analogy with dilute magnetic alloys. In dilute magnetic alloys, partially arranged magnetic atoms interact with each other via RKKY interactions. As mentioned in the introduction, the $J_{\mathrm{eff}}=1$ excitons become a dispersive mode due to strong SE interactions[9]. In this situation, the mobile $J_{\mathrm{eff}}=1$ exciton may behave like a conduction electron. Therefore, the interaction via a mobile $J_{\mathrm{eff}}=1$ exciton between the free spins in a $J_{\mathrm{eff}}=0$ magnet can be regarded as an RKKY interaction. A schematic diagram of this mechanism is shown in Fig. 3. This interaction should be proportional to the concentration of $J_{\mathrm{eff}}=1$, which is consistent with the presence/absence of spin-glass transition. The feasibility of the spin-glass transition in the category of spin–orbit excitonic magnetism is very interesting and requires further theoretical studies. In the broad context, this finding also suggests that the several magnetic responses in $J_{\mathrm{eff}}=0$ magnets, which have been found so far, would be explained by the generated isolated spin model. Thus, we sincerely hope that it should be carefully re-examined.

Summary

We have successfully synthesized new Ru^{4+} double perovskite oxides $SrLaInRuO_6$ and $SrLaGaRuO_6$. The temperature-dependent M/H and isothermal M data can be explained by the van Vleck magnetism of $J_{\mathrm{eff}}=0$ states with additional isolated spins possibly generated by the Ru^{3+}/Ru^{5+} magnetic defects. While $SrLaInRuO_6$ is paramagnetic down to 2 K, $SrLaGaRuO_6$ shows spin-glass transition at $T_f \sim 50$ K. We propose that the origin of spin-glass is isolated spins couple via mobile $J_{\mathrm{eff}}=1$ excitons as an analogy of a dilute magnetic alloy. It is expected that the spin-glass transition due to the introduction of isolated spins demonstrates the existence of mobile $J_{\mathrm{eff}}=1$ excitons as dispersive modes as predicted in spin–orbit-entangled d^4 ions.

Data availability

The datasets generated and analyzed during the current study are available from the corresponding author.

Received: 28 October 2021; Accepted: 27 January 2022
Published online: 14 February 2022

References

1. Kitaev, A. Anyons in an exactly solved model and beyond. *Ann. Phys.* **321**, 2 (2006).
2. Kim, B. J. *et al.* Novel $J_{\mathrm{eff}}=1/2$ Mott state induced by relativestic spin-orbit coupling in Sr_2IrO_4. *Phys. Rev. Lett.* **101**, 076402 (2008).
3. Banerjee, A. *et al.* Proximate Kitaev quantum spin liquid behaviour in a honeycomb lattice. *Nat. Mater.* **15**, 733 (2016).
4. Baek, S.-H. *et al.* Evidence for a field-induced quantum spin liquid in α-$RuCl_3$. *Phys. Rev. Lett.* **119**, 037201 (2017).
5. Kasahara, Y. *et al.* Majonara quantization and half-integer thermal quantum Hall effect in a Kitaev spin liquid. *Nature* **559**, 227 (2018).
6. Kitagawa, K. *et al.* A spin-orbital-entangled quantum liquid on a honeycomb lattice. *Nature* **554**, 341 (2018).
7. Khaliullin, G. Excitonic magnetism in van vleck-type d^4 Mott insulators. *Phys. Rev. Lett.* **111**, 197201 (2013).

8. Chaloupka, J. & Khaliullin, G. Doping-induced ferromagnetism and possible triplet pairing in d^4 Mott insulators. *Phys. Rev. Lett.* **116**, 017203 (2016).
9. Svoboda, C., Randeria, M. & Trivedi, N. Effective magnetic interactions in spin-orbit coupled d^4 Mott insulators. *Phys. Rev. B* **95**, 014409 (2017).
10. Meetei, O. N., Cole, W. S., Randeria, M. & Trivedi, N. Novel magnetic state in d^4 Mott insulators. *Phys. Rev. B* **91**, 054412 (2015).
11. Abragam, A. & Bleaney, B. *Electron Paramagnetic Resonance of Transition Ions* (Clarendon, 1970).
12. Figgis, B. N. & Hitchman, M. A. *Ligand Field Theory and Its Applications* (Wiley-VCH, 2000).
13. Giamarchi, T., Rüegg, C. & Tchernyshyov, O. Bose–Einstein condensation in magnetic insulators. *Nat. Phys.* **4**, 198 (2008).
14. Terzic, J. *et al.* Evidence for a low-temperature magnetic ground state in double perovskite iridates with Ir^{5+} ($5d^4$) ions. *Phys. Rev. B* **96**, 064436 (2017).
15. Phelan, B. F., Seibel, E. M., Badoe, D., Xie, W. & Cava, R. Influence of structural distortions on the Ir magnetism in $Ba_{2-x}Sr_xYIrO_6$ double perovskites. *Solid State Commun.* **236**, 37 (2016).
16. Ranjbar, B. *et al.* Structural and magnetic properties of the iridium double perovskites $Ba_{2-x}Sr_xYIrO_6$. *Inorg. Chem.* **54**, 10468 (2015).
17. Dey, T. *et al.* Ba_2YIrO_6: A cubic double perovskite material with Ir^{5+} ions. *Phys. Rev. B* **93**, 014434 (2016).
18. Cao, G. *et al.* Novel magnetism of Ir^{5+} ($5d^4$) ions in the double perovskite Sr_2YIrO_6. *Phys. Rev. Lett.* **112**, 056402 (2014).
19. Kusch, M. *et al.* Observation of heavy spin-orbit excitons propagating in a nonmagnetic background: The case of $(Ba, Sr)_2YIrO_6$. *Phys. Rev. B* **97**, 064421 (2018).
20. Corredor, L. T. *et al.* Iridium double perovskite Sr_2YIrO_6: A combined structural and specific heat study. *Phys. Rev. B* **95**, 064418 (2017).
21. Laguna-Marco, M. A. *et al.* Magnetism of Ir^{5+}-based double perovskites: Unraveling its nature and the influence of structure. *Phys. Rev. B* **101**, 014449 (2020).
22. Aharen, T. *et al.* Magnetic properties of the $S = 3/2$ geometrically frustrated double perovskites La_2LiRuO_6 and Ba_2YRuO_6. *Phys. Rev. B* **80**, 134423 (2009).
23. Izumi, F. & Momma, K. Three-dimensional visualization in powder diffraction. *Solid State Phenom.* **130**, 15 (2007).
24. Momma, K. & Izumi, F. VESTA 3 for three-dimensional visualization of crystal, volumetric and morphology data. *J. Appl. Crystallogr.* **44**, 1272 (2011).
25. Goto, M., Ueda, H., Michioka, C. & Yoshimura, K. Competition between spin frustration, lattice instability, and the Jahn–Teller effect in $S = 1/2$ geometrically frustrated double perovskite fluorides A_2BTiF_6 (A = K, Rb, Cs; B = Na, K, Rb). *J. Phys. Soc. Jpn* **82**, 104709 (2013).
26. Fan, Z., Sun, K. & Wang, J. Perovskites for photovoltaics: A combined review of organic-inorganic halide perovskites and ferroelectric oxide perovskites. *J. Mater. Chem. A* **3**, 18809–18828 (2015).
27. Brown, I. D. *The Chemical Bond in Inorganic Chemistry: The Bond Valence Model* (Oxford University, 2002).
28. Dass, R. I., Yan, J.-Q. & Goodenough, J. B. Ruthenium double perovskites: Transport and magnetic properties. *Phys. Rev. B* **69**, 094416 (2004).
29. Yoshii, K., Ikeda, N. & Mizumaki, M. Magnetic and dielectric properties of the ruthenium double perovskites La_2MRuO_6 (M = Mg Co, Ni, and Zn). *Phys. Stat. Sol. A* **203**(11), 2812–2817 (2006).
30. Kotani, M. On the magnetic moment of complex ions (I). *J. Phys. Soc. Jpn.* **4**, 293–297 (1949).
31. Lu, H., Chamorro, J. R., Wan, C. & McQueen, T. M. Universal single-ion physics in spin–orbit-coupled d^5 and d^4 ions. *Inorg. Chem.* **57**, 14443–14449 (2018).
32. Martínez, B., Labarta, A., Rodríguez-Solá, R. & Obradors, X. Magnetic transition in highly frustrated $SrCr_8Ga_4O_{19}$: The archetypal *Kagomé* system. *Phys. Rev. B* **50**, 15779 (1994).
33. Kim, B. J. & Khaliullin, G. Resonant inelastic X-ray scattering operators for t_{2g} orbital systems. *Phys. Rev. B* **96**, 085108 (2017).

Acknowledgements

This work was supported by the Japan Society for the Promotion of Science (JSPS) KAKENHI Grants Nos. JP19K14646 and JP21K03441. Part of this work was carried out by the joint research in the Institute for Solid State Physics, the University of Tokyo.

Author contributions

H.Y. conceived and conducted the experiment(s), performed statistical analysis and figure generation, and wrote the original manuscript. Y.H. designed the experiments, conducted the experiment(s), edited the manuscript, and performed statistical analysis. A.M. and K.K. performed the magnetization measurements using pulsed magnetic fields. H.A.K. administrated project and edited the manuscript. All authors discussed the results and reviewed the manuscript.

Competing interests

The authors declare no competing interests.

Additional information

Correspondence and requests for materials should be addressed to Y.H.

Reprints and permissions information is available at www.nature.com/reprints.

Publisher's note Springer Nature remains neutral with regard to jurisdictional claims in published maps and institutional affiliations.